

# Control of a Variable Stiffness Joint for Catching a Moving Object

A. (Ajinkya) Bhole

## Individual Assignment Report

**Committee:**

Dr. R. Carloni  
E. Barrett, MSc  
M. Reiling, MSc

May 2017

008RAM2017  
Robotics and Mechatronics  
EE-Math-CS  
University of Twente  
P.O. Box 217  
7500 AE Enschede  
The Netherlands

Introduction Project (Course Code: 201500140)

# **Control of a Variable Stiffness Joint for Catching a Moving Object**

**By**

Ajinkya Arun Bhole

**Guide: Dr. R. Carloni**

Faculty of Electrical Engineering, Mathematics and  
Computer Science  
University of Twente, The Netherlands

A report submitted in accordance with the  
requirements of the degree MSc. Systems and  
Control

MAY 2016

# Control of a Variable Stiffness Joint for Catching a Moving Object

## Abstract

This work presents a controller design to catch a moving object using a Variable Stiffness Actuator. The controller is designed such that the variable stiffness joint acts as a virtual damper that absorbs the kinetic energy of the moving object. The virtual damping and the output stiffness of the variable stiffness actuator are the control variables.

Two controllers were designed in this work. In the first controller, the damping coefficient of the virtual damper and stiffness of the link joint were kept constant during the course of catching. A major part of this work was done in continuation with the work performed by Julian [10]. The results of this procedure are experimentally validated on the rotational variable stiffness actuator vsaUT-II.

For the second controller, the damping coefficient of the virtual controller as well as the stiffness of the joint were varied along the course of catching. Considering the same control goal which was used in the first controller design, an Optimal Control problem was formulated.

The two controllers were compared in simulations. It was observed that varying the parameters of damping and stiffness provides a betterment in the performance by dampening the motion of the moving object at a faster rate.

# Acknowledgements

I would like to take this opportunity to express profound gratitude and deep regards to **Dr. Raffaella Carloni** for her exemplary guidance, monitoring and constant encouragement throughout the course of this project. The environment created at the **Robotics and Mechatronics Lab** at University of Twente is probably the best a student interested in robotics could ever hope for.

Working on this project was a challenging and an interesting adventure and I enjoyed having great colleagues and friends, **Mark, Eamon, Mohsen, Rene and Clevi** who were always there to help me with my work.

# Contents

<b>1</b>	<b>Introduction</b>	<b>7</b>
<b>2</b>	<b>Controller 1</b>	<b>9</b>
2.1	Controller Design . . . . .	9
2.1.1	Desired behavior and control goals . . . . .	9
2.1.2	Control architecture . . . . .	10
2.1.3	Damping coefficient . . . . .	11
2.1.4	Stiffness adaptation . . . . .	13
2.2	Experiments . . . . .	15
2.2.1	Experimental set-up . . . . .	15
2.2.2	Results . . . . .	18
<b>3</b>	<b>Controller 2</b>	<b>22</b>
3.1	Optimal Control Problem Formulation . . . . .	22
3.2	Implementation using TOMLAB Toolbox . . . . .	23
3.3	Comparison of results with Controller 1 . . . . .	27
3.4	Conclusion from Simulation Results . . . . .	31
<b>4</b>	<b>Discussion and Future Work</b>	<b>32</b>

# List of Figures

1.1	Tasks involving adjustment of the dynamic characteristics of musculoskeletal system. . . . .	7
2.1	A generic variable stiffness actuator – $J_{load}$ is the inertia of the load, $K(q_1)$ is the output stiffness of the VSA, $\dot{q}_1$ and $\dot{q}_2$ , are the angular velocities, as imposed by the two internal motors, and $\dot{r}$ is the angular velocity of the load. . . . .	9
2.2	Illustration of a virtual damper with the damping coefficient $c_v$ replacing the motor for changing the angle $q_2$ in order to design a controller that acts as a damper. The motor for changing the angle $q_1$ is irrelevant for this part and, therefore, taken out of the sketch. . . . .	11
2.3	Block diagram based on the illustration of Figure 2.2. . . . .	11
2.4	Comparison of position of $r$ for a critically damped case, i.e., $\zeta = 1$ , and over-damped case, i.e., $\zeta = 1.1$ . . . . .	12
2.5	Position of $r$ and $q_2$ for critically damped case, i.e., $\zeta = 1$ . . . . .	13
2.6	Position of $r$ and $q_2$ for under-damped case, i.e., $\zeta = 0.7$ . . . . .	13
2.7	Position control on $q_1$ for achieving $K_d$ . . . . .	15
2.8	The vsaUT-II variable stiffness actuator [7] – The labels indicate 1) the output joint, 2) the actuator frame, 3) the lever arm and gears mechanism, 4) the motor for changing the output position $q_2$ , 5) timing belt transmission and 6) motor for varying the pivot point position $q_1$ and, therefore, the output stiffness. . . . .	16
2.9	Experimental set-up: the object (1) rolls down from the ramp (2), hits the magnet (3), which is rigidly connected to the joint (4) actuated by the VSA (5). . . . .	17
2.10	Validation of simulation on experimental set up at an uncontrolled system. The iron ring hits the VSA output at $t = 17.3$ s. . . . .	18

2.11 Simulation and experiments are performed at a constant stiffness of 1.5Nm/rad and a damping ratio of  $\zeta = 1$ . The behavior of the simulated  $r(t)$  (desired link position) is compared to to the experimental data from the set up (actual link position). . . . . 18

2.12 Simulation and experiments are performed at a constant stiffness of 1.5Nm/rad and a damping ratio of  $\zeta = 1$ . The behavior of the simulated  $q_2(t)$  (commanded motor position) is compared to the experimental data from the set up (motor position). . . . . 19

2.13 Simulation and experiments are performed at a constant stiffness of 1.5Nm/rad and a damping ratio of  $\zeta = 0.7$ . The behavior of the simulated  $r(t)$  (desired link position) is compared to the experimental data from the set up (actual link position). . . . . 20

2.14 Simulation and experiments are performed at a constant stiffness of 1.5Nm/rad and a damping ratio of  $\zeta = 0.7$ . The behavior of the simulated  $q_2(t)$  (commanded motor position) is compared to the experimental data from the set up (motor position). . . . . 20

3.1 Link Velocity vs Time (Keeping damping and Stiffness Constant) . . 27

3.2 Link Position vs Time (Keeping damping and Stiffness Constant) . . 28

3.3 Deviation  $r - q_2$  vs Time (Keeping damping and Stiffness Constant) . 28

3.4 Link Velocity vs Time (Varying damping and Stiffness Constant) . . 28

3.5 Link Position vs Time (Varying damping and Stiffness Constant) . . 29

3.6 Deviation  $r - q_2$  vs Time (Varying damping and Stiffness Constant) . 29

3.7 Link Stiffness vs Time (Varying damping and Stiffness Constant) . . 29

3.8 Damping vs Time (Varying damping and Stiffness Constant) . . . . 30

3.9 Acceleration vs Time (Varying damping and Stiffness Constant) . . 30

# Chapter 1

## Introduction



Figure 1.1: Tasks involving adjustment of the dynamic characteristics of musculoskeletal system.

Shown in Figure 1.1 are some of the skillful movements like throwing, running and hammering. Humans perform skillful movements by adjusting the dynamic characteristics of their musculoskeletal system. Taking this strategy as an inspiration, roboticists are trying to integrate such skillful capabilities into robotic manipulators. Making use of special type of actuators like the Variable Stiffness Actuators (VSAs) is bringing them closer to realize this goal.

Recent developments in the fields of physical human-robot interaction and robot-environment interaction have brought to the realization of robots that implement variable stiffness actuators (VSAs) [2, 5, 14, 6], and to the design of controllers that allows such robotic systems to mimic the features of the human muscles [3].

This work presents the design of a controller for a one degree of freedom joint, actuated by a VSA, that should catch a moving object. The control architecture of the Variable Stiffness Joint (VSJ) is inspired by the human behavior. More specifically, when humans catch a moving object, the arm muscles are first pre-tensioned for preparing the arm to the impact. Then, when the arm gets into contact with the object, the muscles absorb the kinetic energy of the moving object.



In this work, the VSA is controlled so that the attached joint behaves as a virtual damper that absorbs the kinetic energy of the moving object. It is assumed that the mass of the moving object is known *a priori* and a mechanism is implemented at the VSJ that rigidly latches the object to the VSJ after collision. Moreover, the moving object is not tracked with a vision system nor is detected with sensors before or after it collides with the VSJ.

The task of catching a falling object has been already addressed in the literature. In [13], the task relies on the use of a position tracking controller that tracks a desired trajectory before the contact between the object and the end-effector occurs. The work in [4] discusses the optimal catching point but do not discuss about the choice of impedance parameters used to impede the object after impact. The work in [9] shows an optimal control of a simulated series impedance actuator while catching an object. In this work, similarly to [11], the controller is tuned to obtain a desired damping behavior of the VSJ. However, in [11], the controller acts as a pure damper and, therefore, it only absorbs the kinetic energy generated by the impact of the moving object. In [12] and [1], control methods based on damping injection have been used. Similarly to [1], in this work, the damping coefficient is scheduled on both the stiffness and the inertia of the system but the control gains in [1] are scheduled according to the desired dynamics of a linearized system.

This report presents two controllers:

- Controller 1: This controller keeps the damping coefficient of the virtual damper and stiffness of the link joint constant during the course of catching
- Controller 2: Here, the damping coefficient of the virtual controller as well as the stiffness of the joint are varied along the course of catching.

# Chapter 2

## Controller 1

This chapter discusses the design, implementation and validation of Controller 1 discussed in the Introduction. This chapter is majorly adopted from the work performed by Julian [10].

### 2.1 Controller Design

In this section, the design of a controller for a VSJ is presented. VSAs have the advantage that their output stiffness can be changed independently of the output position. In this work, a VSA is considered which consists of two internal motors, an elastic element and an output where a load, i.e., the joint, can be connected to, as shown in Figure 2.1. In this configuration, one motor (whose position is indicated by the angle  $q_2$ ) changes the position of the load via an elastic element. The other motor (whose position indicated by the angle  $q_1$ ) tunes the output stiffness  $K(q_1)$ . The joint has inertia  $J_{load}$  and its position is indicated by the angle  $r$ .

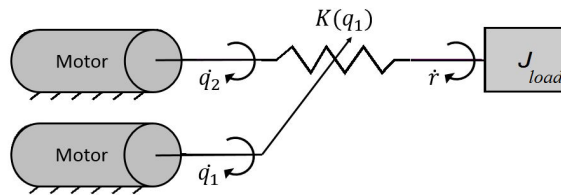


Figure 2.1: A generic variable stiffness actuator –  $J_{load}$  is the inertia of the load,  $K(q_1)$  is the output stiffness of the VSA,  $\dot{q}_1$  and  $\dot{q}_2$ , are the angular velocities, as imposed by the two internal motors, and  $\dot{r}$  is the angular velocity of the load.

#### 2.1.1 Desired behavior and control goals

The control goal is to catch a moving object with the VSJ described above while mimicking the human behavior. The mass of the object is known while its velocity

towards the VSJ is unknown. When the object impacts the VSJ, the inertia of the output increases. Conservation of angular momentum can be used to find the initial angular velocity imparted to the link by the hitting object.

For a successful catch, the object must not bounce back and loose contact with the link i.e. the spring must always remain in compressed state (i.e.,  $r - q_2$  must be positive).

Also, in order to allow for absorption of the impact and avoid bouncing back of the object, the initial setting of the output stiffness of the VSJ should be as low as possible. Moreover, the deflection of  $r$  from its initial position should be small so that the object is stopped with a low deflection and also in order to take into account the physical constraints of the VSJ. Therefore, to satisfy these requirements, the following control goals are defined:

- $\lim_{t \rightarrow t_f} \dot{r}(t) = 0$ , i.e., the kinetic energy of the link should be absorbed
- $r - q_2 > 0$ , i.e., the object should not bounce on the joint and, thus, there is no loss of contact between the object and the link
- $|r(0) - r(t_f)|$  low and within the physical constraints of the VSJ ( $0$  and  $t_f$  are the initial and final instants of time of the catching task)
- $K(q_1, t)$  as low as possible  $\forall t \in [0, t_f]$

The procedure for the attainment of the above-mentioned control goals is explained in the following sections.

### 2.1.2 Control architecture

The first control goal  $\lim_{t \rightarrow t_f} \dot{r}(t) = 0$  imposes that the kinetic energy of the link is absorbed. to achieve this goal, the motor that moves the VSJ is controlled to behave as a virtual damper. This scenario is shown in Figure 2.2, where the motor that changes the angle  $q_2$  is sketched as a damper with a damping constant  $c_v$ . In the figure, the circle represents the moving object that should be caught. The parameters for the moving object are its mass  $m_{obj}$  and its velocity  $v_{obj}$ . The moving object provides an angular impulse  $M_{obj}$  to the link. It follows that the controlled system is described by the following equations:

$$J\ddot{r} + K(r - q_2) = M_{obj}\delta(t)$$

$$c_v\dot{q}_2 = K(r - q_2)$$

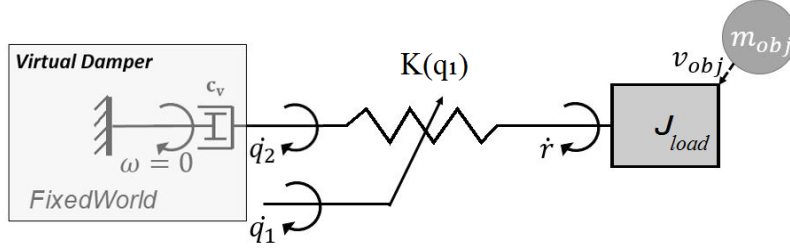


Figure 2.2: Illustration of a virtual damper with the damping coefficient  $c_v$  replacing the motor for changing the angle  $q_2$  in order to design a controller that acts as a damper. The motor for changing the angle  $q_1$  is irrelevant for this part and, therefore, taken out of the sketch.

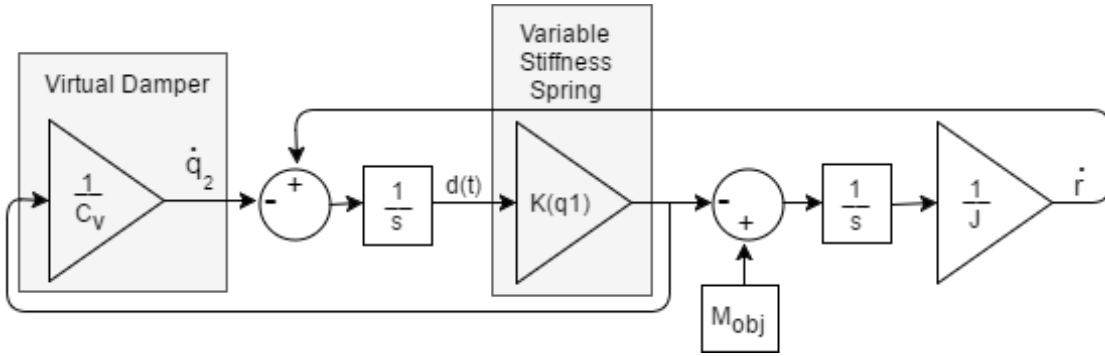


Figure 2.3: Block diagram based on the illustration of Figure 2.2.

where  $J$  is the combined inertia of the VSJ link along with the impacting object (i.e.  $J_{load} + J_{obj}$ ) and  $\delta(t)$  is the Dirac delta function.

Based on the above equations, a block diagram, as depicted in Figure 2.3, can be drawn. The block diagram shows that the controller implements a virtual damper and is realized with a proportional controller with a gain of  $1/c_v$ . The input of the controller is the torque at the elastic element after the impact, which results out of the angle difference  $r - q_2$  and the stiffness  $K(q_1)$  of the VSJ. The output of the controller is a target velocity  $\dot{q}_2$  for the motor. The velocity  $\dot{r}$  of the VSJ results from the torque at the the elastic element and the angular impulse  $M_{obj}$  acting on the inertia of the VSJ.

### 2.1.3 Damping coefficient

By analyzing the block diagram in Figure 2.3, the transfer function from the momentum of the moving object  $M_{obj}$  to the velocity of the VSA output  $\dot{r}$  is :

$$\frac{\dot{r}(s)}{M_{obj}} = \frac{1}{J} \frac{s + \frac{K}{c_v}}{s^2 + s\frac{K}{c_v} + \frac{K}{J}}$$

The natural frequency  $\omega$  of the system is given by

$$\omega = \sqrt{\frac{K}{J}} \quad (2.1)$$

while the damping ratio is given by

$$2\zeta\omega = \frac{K}{c_v} \quad (2.2)$$

By substituting equation 2.1 in 2.2, it follows that

$$\zeta = \frac{\sqrt{KJ}}{2c_v}$$

that yields to:

$$c_v = \frac{\sqrt{KJ}}{2\zeta} \quad (2.3)$$

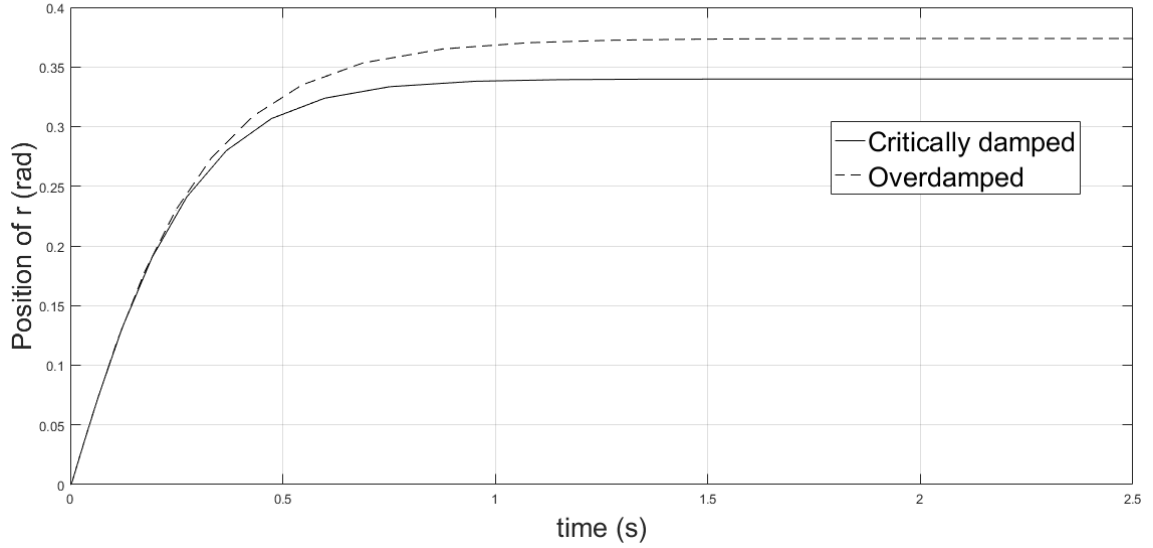


Figure 2.4: Comparison of position of  $r$  for a critically damped case, i.e.,  $\zeta = 1$ , and over-damped case, i.e.,  $\zeta = 1.1$ .

Figure 2.4 shows a simulation comparing a critically-damped and over-damped case. As it can be seen, the final value of  $r$  (i.e.  $|r(0) - r(t_f)|$ , when  $r(0) = 0$ ) is greater in an over-damped case than in the critically damped case. Therefore, critically damped case is preferred over an over-damped case. Figures 2.5 and 2.6 show the comparison of the positions of  $r$  and  $q_2$  for critically-damped and under-damped case. As it can be seen from the figures, the value of the spring deflection  $r - q_2$  always remains positive for critically damped case which is not the case with under-damped system. Therefore, the critically damped case allows catching

without bouncing of the object and, thus, without any loss of contact between the object and the link.

In order to have a critically damped system,  $\zeta$  should be equal to 1. Therefore, since the output stiffness of a VSA can vary, i.e.,  $K(q_1)$ , the damping factor  $c_v$  in equation 2.3 should be scheduled on both the stiffness and the inertia of the system.

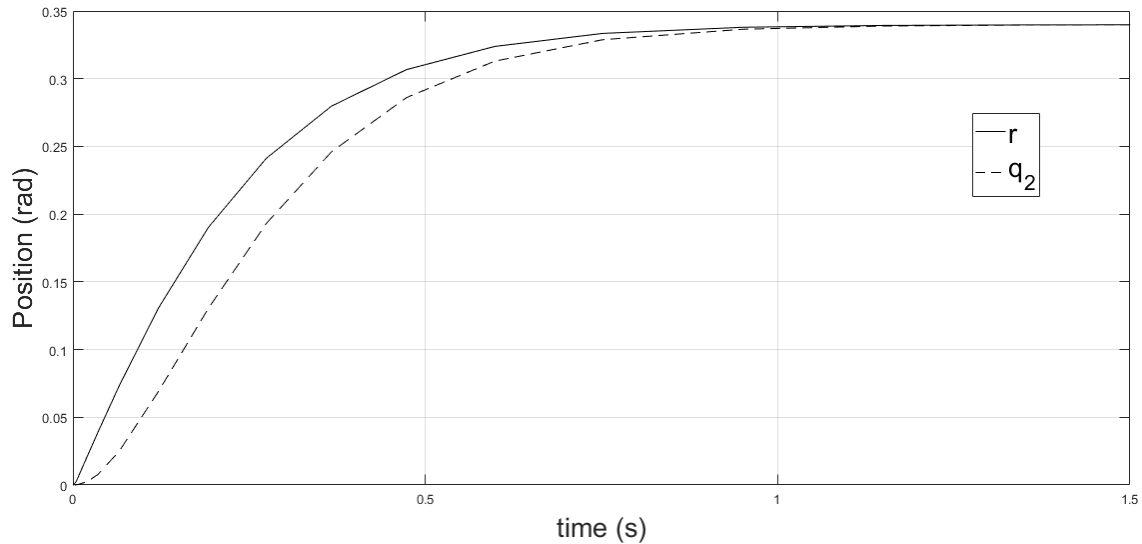


Figure 2.5: Position of  $r$  and  $q_2$  for critically damped case, i.e.,  $\zeta = 1$ .

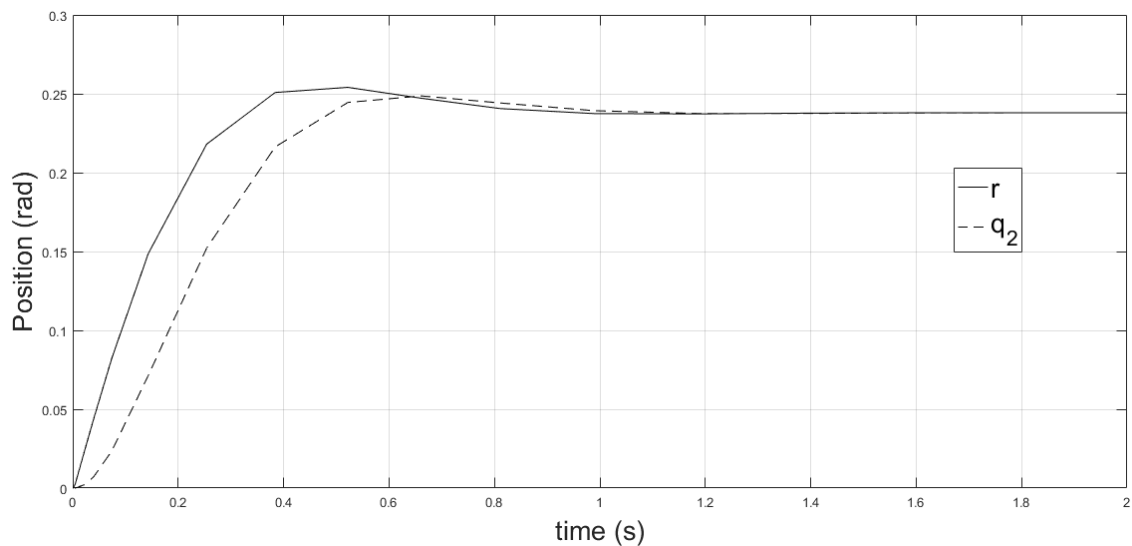


Figure 2.6: Position of  $r$  and  $q_2$  for under-damped case, i.e.,  $\zeta = 0.7$ .

### 2.1.4 Stiffness adaptation

The control goal, according which  $K(q_1)$  should be low, allows for the absorption of the impact. The stiffness is adapted such that the deflection  $r(t_f) - r(0)$  does not

exceed a maximum defined deflection  $r_{lim}$ . The following procedure explicates this adaptation.

By analyzing the block diagram in Figure 2.3, we have:

$$\frac{r(s)}{M_{obj}} = \frac{s + 2\omega}{Js(s + \omega)^2}$$

This results in the following equation:

$$r(t) = \frac{M_{obj}}{J} \left( \frac{2}{\omega} - \frac{2}{\omega} e^{-\omega t} - t e^{-\omega t} \right)$$

The maximum of  $r(t)$  occurs as  $t \rightarrow \infty$

$$\lim_{t \rightarrow \infty} r(t) = \frac{2M_{obj}}{Ja} = \frac{2M_{obj}}{\sqrt{KJ}}$$

Thus, we have,

$$\frac{2M_{obj}}{\sqrt{KJ}} \leq r_{lim}, \quad \text{i.e.,} \quad \frac{4M_{obj}^2}{r_{lim}^2 J} \leq K$$

Due to mechanical constraints on the VSJ setup used for the experiments, the value of deflection  $d(t)$  (i.e.  $r(t) - q_2(t)$ ) is constrained within a certain range  $-d_{lim}$  and  $d_{lim}$ . Thus, the minimum stiffness required to keep this deflection within this range is also considered.

By analyzing the block diagram in Figure 2.3, we have:

$$\frac{d(s)}{M_{obj}} = \frac{1}{J} \frac{1}{(s + a)^2}$$

Thus, we have:

$$d(t) = \frac{M_{obj}}{J} (t e^{-at}) \tag{2.4}$$

The maximum of  $d(t)$  occurs at  $t = \frac{1}{a}$ . Thus, we have:

$$\frac{M_{obj}}{e\sqrt{KJ}} \leq d_{lim} \quad \text{i.e.,} \quad \frac{M_{obj}^2}{e^2 d_{lim}^2 J} \leq K$$

Thus, we choose:

$$K = \max \left( \frac{4M_{obj}^2}{r_{lim}^2 J}, \frac{M_{obj}^2}{e^2 d_{lim}^2 J} \right)$$

Since the stiffness  $K(q_1)$  is a function of  $q_1$ , a desired output stiffness  $K_d$  defines a desired  $q_{1d}$ . This leads to a position controller on  $q_1$ , as shown in Figure 2.7. The first block transforms a desired stiffness  $K_d$  into a desired position of the pivot point  $q_{1d}$ . After this block there is a closed loop containing the position controller and the

motor whose position is indicated by the angle  $q_1$ .

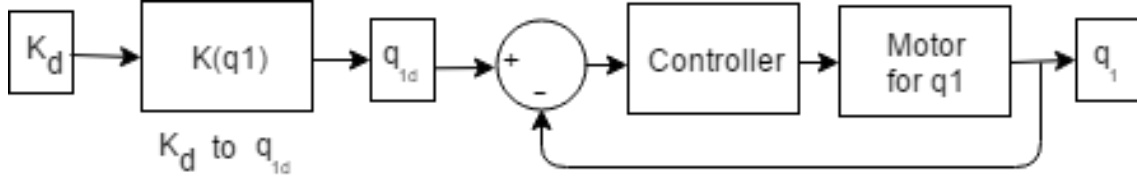


Figure 2.7: Position control on  $q_1$  for achieving  $K_d$ .

## 2.2 Experiments

In this section, the proposed controller is implemented on the rotational variable stiffness actuator vsaUT-II, depicted in Figure 2.8 [7], for experimental validation.

### 2.2.1 Experimental set-up

The mechanical design of the vsaUT-II is such that the output stiffness can be varied by changing the transmission ratio between the internal linear springs and the output. The variable transmission is obtained by means of a lever arm with variable effective length, realized by moving a pivot point along the lever arm.

As extensively described in [7], the position of the pivot point along the lever arm is defined by the internal motor  $q_1$ , which spans from 0 to  $L$ . More precisely, the motion of the pivot is actuated by the internal motor  $q_1$ , of which the output rotation is converted into a linear pivot motion along the lever via a 1 : 2 planetary gear set. The deflection of the lever arm when the springs are not loaded is defined by the motor  $q_2$ . More precisely, the motor  $q_2$  defines the position of the actuator frame (see label 2 in Figure 2.8). This implies that, if the internal springs are loaded, the output position  $r$  of the actuation system is different than the position of the actuator frame  $q_2$ . The output stiffness  $K$  is

$$K := \frac{\partial \tau_r}{\partial r} = 2k \frac{L^2}{q_1^2} (L - q_1)^2 \cos(2(r - q_2))$$

where  $k$  is the elastic constant for the internal springs.

An initial stiffness of 1Nm/rad was chosen so that the natural frequency of the system  $\omega$  is smaller than the crossover frequency of the system  $w_c$  for changing the position of  $q_2$  and, therefore, being able to follow the movement of  $r$ . Due to mechanical end-stops of the system,  $q_2 = [-0.5, \dots, 0.5]$ rad and  $r = [q_2 - 0.7, \dots, q_2 + 0.7]$ rad. Further important values for creating a model of the VSJ and for implementing the controller are reported in Tables 2.1 - 2.3.



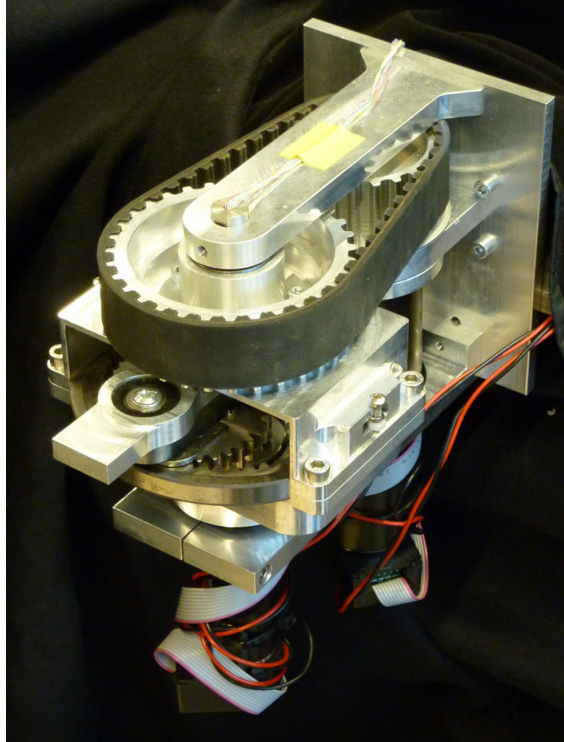


Figure 2.8: The vsaUT-II variable stiffness actuator [7] – The labels indicate 1) the output joint, 2) the actuator frame, 3) the lever arm and gears mechanism, 4) the motor for changing the output position  $q_2$ , 5) timing belt transmission and 6) motor for varying the pivot point position  $q_1$  and, therefore, the output stiffness.

Table 2.1: Parameters of drivetrain for degree of freedom  $q_1$ .

max. motor speed	872 [rad s]
max. continuous torque	0.0263 [Nm]
stall torque	0.243 [Nm]
speed reduction ratio	0.0022 [–]
motor shaft inertia	$1.07 \cdot 10^{-6}$ [kg m <sup>2</sup> ]
motor friction	$6.4 \cdot 10^{-6}$ [Ns/m]
transmission input inertia	$4 \cdot 10^{-8}$ [kg m <sup>2</sup> ]
max. transmission efficiency	0.59 [–]

Table 2.2: Parameters of drivetrain for degree of freedom  $q_2$ .

max. motor speed	726 [rad/s]
max. continuous torque	0.17 [Nm]
stall torque	2.28 [Nm]
speed reduction ratio	0.0044 [–]
motor shaft inertia	$1.38 \cdot 10^{-5}$ [kg m <sup>2</sup> ]
motor friction	$3 \cdot 10^{-6}$ [Ns/m]
transmission input inertia	$9.1 \cdot 10^{-7}$ [kg m <sup>2</sup> ]
max. transmission efficiency	0.72 [–]

Table 2.3: Parameters for the transmission between  $q_2$  and  $r$ .

friction	$1.2 \cdot 10^{-2}$ [Ns/m]
inertia	$1.1 \cdot 10^{-2}$ [kg m <sup>2</sup> ]

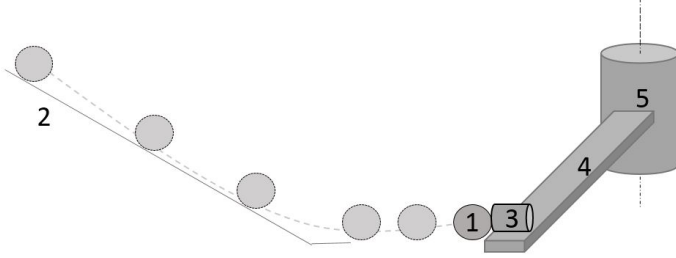


Figure 2.9: Experimental set-up: the object (1) rolls down from the ramp (2), hits the magnet (3), which is rigidly connected to the joint (4) actuated by the VSA (5).

A magnet has been mounted on the VSJ for rigidly latching the object to the joint. The object is an iron ring, with a weight of  $m_{obj} = 0.108\text{kg}$ , rolling down from a ramp before hitting the output. The iron ring hits the output at  $t = 1\text{s}$ . If the iron ring is connected to the output the inertia of the VSA output changes to  $0.0205\text{kg} \cdot \text{m}^2$ . The experimental set-up is schematically shown in Figure 2.9, where (1) is the object rolling down from the ramp (2) and hitting the magnet (3), which is rigidly connected to the joint (4) actuated by the VSA (5).

The VSA is equipped with three position sensors for measuring  $q_1$ ,  $q_2$  and  $r$ . An Arduino  $\mu$ -controller (Arduino AG, Italy) communicates to the sensors and actuators. This  $\mu$ -controller has an interface to Matlab-Simulink (Mathworks, USA) so that the controller can be implemented in Matlab-Simulink. The motor controller for  $q_1$  and  $q_2$  are ELMO Whistle miniature digital servo drives (SimplIQ Whistle, Elmo Motion Control Ltd., The Netherlands).

The limitations of the system are the end-stops of  $q_2$  and  $r$ , and the maximum motor speed of  $q_1$  and  $q_2$ . The end-stops limit the movement of the VSA output. The maximum motor speed for  $q_2$  limits the maximum damping factor of the virtual damper and the maximum motor speed for  $q_1$  limits the rate of change for the stiffness of the elastic element. The experiments described in this work were performed within the limitations of the system.

## 2.2.2 Results

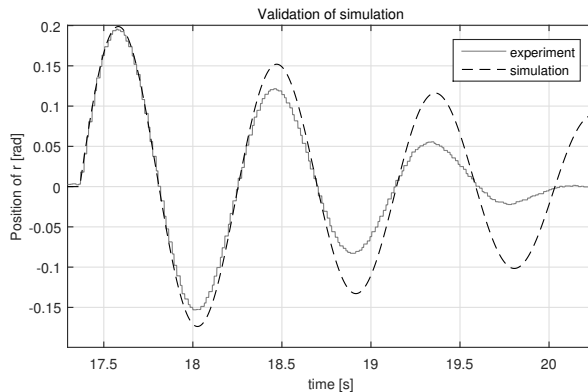


Figure 2.10: Validation of simulation on experimental set up at an uncontrolled system. The iron ring hits the VSA output at  $t = 17.3$  s.

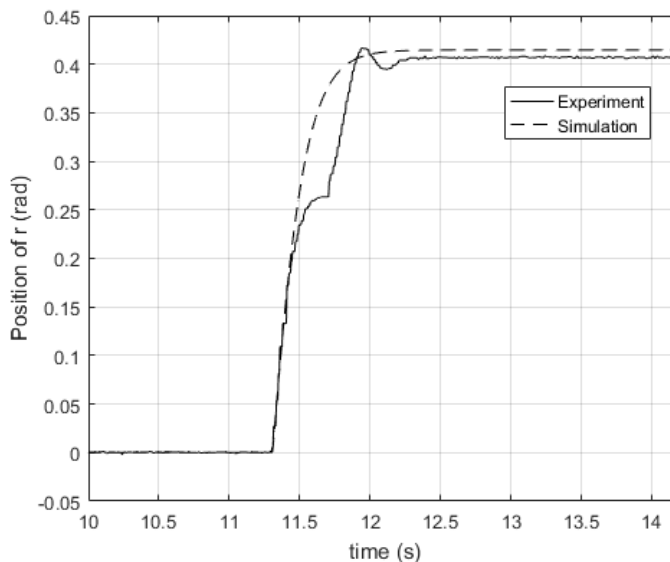


Figure 2.11: Simulation and experiments are performed at a constant stiffness of  $1.5\text{Nm/rad}$  and a damping ratio of  $\zeta = 1$ . The behavior of the simulated  $r(t)$  (desired link position) is compared to to the experimental data from the set up (actual link position).

In this section, the proposed controller is validated in both simulations and experiments. First, the behavior of the uncontrolled system of the experimental set up was compared to the simulation at a stiffness of  $1.5\text{ Nm/rad}$  while the virtual damper was inactive ( $\dot{q}_2 = 0\text{ rad/s}, \forall t \in [0, t_f]$ ). The results are shown in Figure 2.10. While the simulation and the experiment show similar oscillation behavior, differences in the damping behavior can be seen. For the simulation, a simplified friction model with constant friction is modeled which leads to these differences. The validation of the

simulation model provides good insight for implementing and testing the controller in a simulation before applying it to the experimental set up.

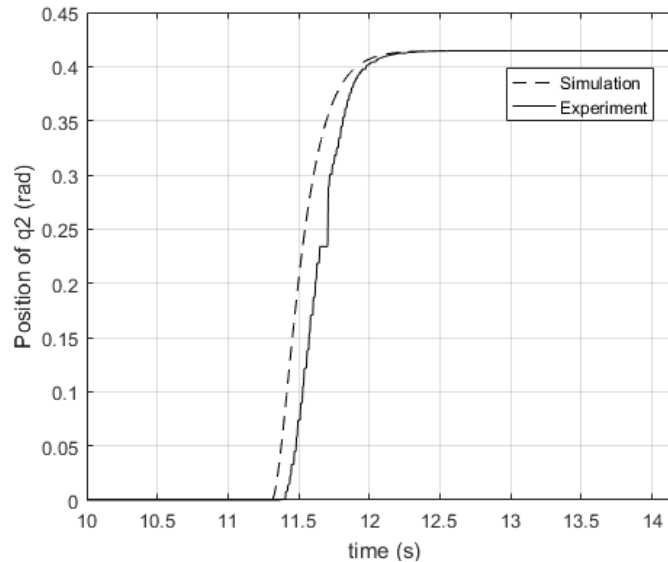


Figure 2.12: Simulation and experiments are performed at a constant stiffness of  $1.5\text{Nm/rad}$  and a damping ratio of  $\zeta = 1$ . The behavior of the simulated  $q_2(t)$  (commanded motor position) is compared to the experimental data from the set up (motor position).

The second experiment, shown in Figure 2.11-2.12, was performed by implementing the virtual damper. The behavior of a critically damped system was analyzed in both simulations and on the experimental set up. The stiffness of the elastic element has been set at a constant value of  $1.5\text{Nm/rad}$ . A damping ratio of  $\zeta = 1$  results in a damping coefficient for the virtual damper of  $c_v = 0.0877\text{ Nms/rad}$ . As it can be seen in Figure 2.11, for a small time just after the impact, the link position follows the simulated link position, but subsequently it starts deviating from it. The reason for this can be seen from Figure 2.12, where it can be noted that there is a time delay between the commanded motor position (simulation) and the actual motor position (experiment). The cause for time delay is the communication between Matlab-Simulink, the Arduino  $\mu$ -controller, and Elmo motor controllers. This delay results in incomplete dissipation of the energy of the link which can be seen in form of small oscillations towards the end, which finally die out due to internal friction.

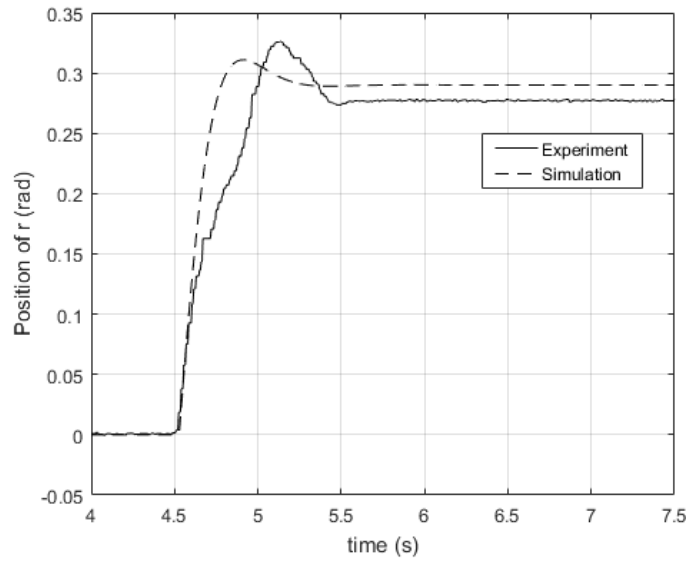


Figure 2.13: Simulation and experiments are performed at a constant stiffness of  $1.5\text{Nm/rad}$  and a damping ratio of  $\zeta = 0.7$ . The behavior of the simulated  $r(t)$  (desired link position) is compared to the experimental data from the set up (actual link position).

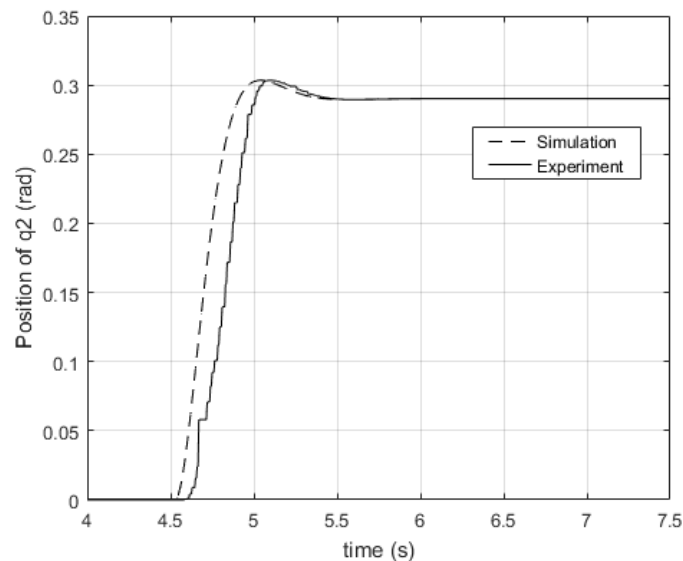


Figure 2.14: Simulation and experiments are performed at a constant stiffness of  $1.5\text{Nm/rad}$  and a damping ratio of  $\zeta = 0.7$ . The behavior of the simulated  $q_2(t)$  (commanded motor position) is compared to the experimental data from the set up (motor position).

Varying the damping ratio should have an influence on the coefficient of the virtual damper. Therefore, experiments were performed with slightly changed damping coefficients and the behavior is compared to the critically damped system. The behavior of an under-damped system was analyzed on the experimental set up and in

a simulation. The stiffness of the elastic element is constant at 1.5Nm/rad during this experience. A damping ratio of  $\zeta = 0.7$  results in a damping coefficient for the virtual damper of  $c_v = 0.1253$  Nms/rad. As it can be seen in Figure 2.13, for a small time just after the impact, the actual link position follows the desired link position, but subsequently it starts deviating from the desired link position. The reason being similar to that of the critically-damped experiment. As it can be seen in Figure 2.14, there is a time delay between the commanded motor position and the actual motor position.

The results demonstrate that the implementation of a virtual damper for controlling a VSA leads to a definable catching behavior of an object within the system limitations. The deviations from desirable results occurred because of the time delays in communication between Matlab-Simulink, the Arduino  $\mu$ -controller, and the ELMO motor controllers.

# Chapter 3

## Controller 2

This chapter discusses the design of Controller 2, in which the damping coefficient of the virtual controller as well as the stiffness of the joint are varied along the course of catching.

### 3.1 Optimal Control Problem Formulation

To formulate an optimal control problem we firstly look at the control goal. The control goal is to stop the object as quickly as possible and with as low deflection as possible.

Some of the clear constraints of the problem are presented firstly, which will make the understanding of the cost function of the optimal problem easier.

We have

$$\ddot{r} \leq 0$$

$$0 \leq |\dot{r}| \leq |v_{ini}| \quad (3.1)$$

Now, to stop the object as quickly as possible and with as low deflection as possible, it is clear from the above constraints that the deceleration should be maximized.

The other constraints being the dynamics of the system, the initial and final constraints and the system constraints.

The optimal control problem is thus formulated as follows:

- States:  $\ddot{r}, \dot{r}, r, q_2, k$
- control inputs:  $c_v$  and  $\dot{k}$

$$\begin{aligned}
 & \text{minimize} && \int_0^{t_f} -(\ddot{r})^2 dt \\
 & \text{subject to} && J\ddot{r} = \dot{k}(r - q_2) + k(\dot{r} - \dot{q}_2) \\
 & && J\ddot{r} = k(r - q_2) \\
 & && c_v\dot{q}_2 = k(r - q_2) \\
 & && \dot{r}(0) = v_{ini} \\
 & && \dot{r}(t_f) = 0 \\
 & && 0 \leq |\dot{r}| \leq |v_{ini}| \\
 & && \ddot{r} \leq 0 \\
 & && \ddot{r}(t_f) = 0 \\
 & && -0.5 \leq q_2 \leq 0.5 \\
 & && 0 \leq r - q_2 \leq 0.7 \\
 & && k_{min} \leq k \leq k_{max} \\
 & && -\dot{k}_{max} \leq \dot{k} \leq \dot{k}_{max} \\
 & && -\dot{q}_{2max} \leq \dot{q}_2 \leq \dot{q}_{2max} \\
 & && 0 \leq c_v \leq \frac{\sqrt{k_{max}J}}{2}
 \end{aligned}$$

where,  $k_{min}$  and  $k_{max}$  are the minimum and maximum stiffness the variable stiffness joint can achieve.  $\dot{k}_{max}$  is the maximum rate at which stiffness can be varied, which depends on the maximum speed of the motor changing the stiffness.  $\dot{q}_{2max}$  is the maximum rate at which  $q_2$  can be varied.

## 3.2 Implementation using TOMLAB Toolbox

The TOMLAB toolbox PROPT [8] was used for solving the posed optimal control problem. Following is the MATLAB code:

```

1 %% Optimal Catching
2
3 %% Problem setup
4 toms t
5 toms t_f;
6 m=0.02;
7 nvec = [100 105 110 115 120]; %105 110 115 120
8 vini=2;
9 stiffini=1;
    
```



```
10
11 for i=1:length(nvec)
12
13     n = nvec(i);
14     p = tomPhase('p', t, 0, t_f, n);
15     setPhase(p);
16
17
18     tomStates x1 x2 x3 x4 x5 x6 x7
19     tomControls u1 u2
20
21     % Initial guess
22     % Note: The guess for t_f must appear in the list before
23           expression involving t.
24     if i==1
25         x0 = {t_f == 5
26             icollocate({
27                 x1 == vini
28                 x2 == 0
29                 x3 == 0
30                 x4 == stiffini
31                 x5 == 0
32             })
33         collocate({u1==0
34                 u2==0
35             })
36     else
37         x0 = {t_f == tf_init
38             icollocate({
39                 x1 == x1_init
40                 x2 == x2_init
41                 x3 == x3_init
42                 x4 == x4_init
43                 x5 == x5_init
44             })
45         collocate({u1==u1_init
```

```

46     u2==u2_init
47     })
48     };
49     end
50     % Box constraints
51     cbox = {0.01 <= t_f <= 100
52           -0.7 <= mcollocate(x2-x3) <= 0.7
53           -1 <= mcollocate(x3) <= 1
54           stiffini <= mcollocate(x4) <= 500
55           0 <= mcollocate(x1) <= vini
56           -1000 <= mcollocate(x6) <= 0%0 <= icollocate(x4*(x2-
           x3)/m) <= 1000
57           0.1 <= collocate(u1) <= 2
58           -20 <= collocate(u2) <= 20};
59
60     % Boundary constraints
61     cbnd = {initial({x1 == vini; x2 == 0; x3 == 0; x4 ==
           stiffini; x5 ==0})
62           final({x1 == 0; x6 == 0})};
63
64     % ODEs and path constraints
65     ceq = collocate({
66         dot(x1) == -x4*(x2-x3)/m
67         dot(x2) == x1
68         dot(x3) == x4*(x2-x3)/u1
69         dot(x4) == u2
70         dot(x5) == (x2-x3)^2
71         dot(x6) == -(u2*(x2-x3)+x4*(x1-(x4*(x2-x3)/u1)))/m
72         dot(x7) == -x6^2
73     });
74
75     % Objective
76     objective = final(x7);
77
78     %% Solve the problem
79     %Prob.SOL.optPar(30) = 3000;
80     options = struct;
    
```

```
81     options.name = 'SEA';
82     solution = ezsolve(objective, {cbox, cbnd, ceq}, x0,
        options);
83     x1_init = subs(x1, solution);
84     x2_init = subs(x2, solution);
85     x3_init = subs(x3, solution);
86     x4_init = subs(x4, solution);
87     x5_init = subs(x5, solution);
88     u1_init = subs(u1, solution);
89     u2_init = subs(u2, solution);
90     tf_init = subs(tf, solution);
91 end
92
93 %% Plot the result
94 time=0:solution.tf/nvec(end):solution.tf;
95 time=time';
96 timeu=time(2:end);
97
98 figure;
99 plot(time, solution.x1_p)
100 title('EE_velocity vs time')
101
102 figure;
103 plot(time, solution.x2_p)
104 title('EE_position vs time')
105
106 figure;
107 plot(time, solution.x3_p)
108 title('Motor Position vs time')
109
110 figure;
111 plot(time, solution.x4_p)
112 title('Stiffness vs time')
113
114 figure;
115 plot(time, solution.x2_p-solution.x3_p)
116 title('Deviation vs time')
```

```
117
118     figure ;
119     plot (timeu , solution . u1_p)
120     title ( 'Damping vs time ' )
121
122     figure ;
123     plot (timeu , solution . u2_p)
124     title ( 'Stiffness speed vs time ' )
125
126     figure ;
127     plot (time , solution . x6_p)
128     title ( 'EE Acc. vs time ' )
```

### 3.3 Comparison of results with Controller 1

The results using the optimal control framework (Controller 2) used are compared to that using Controller 1 using Simulations. For this, an impulse was applied to the link giving it an initial velocity of  $1 \text{ rad/s}$ . Figures 3.1-3.3 show the results obtained if the damping and stiffness are kept constant, while Figures 3.4-3.9 show the results obtained by varying the stiffness and damping using the optimal control framework (Controller 2).

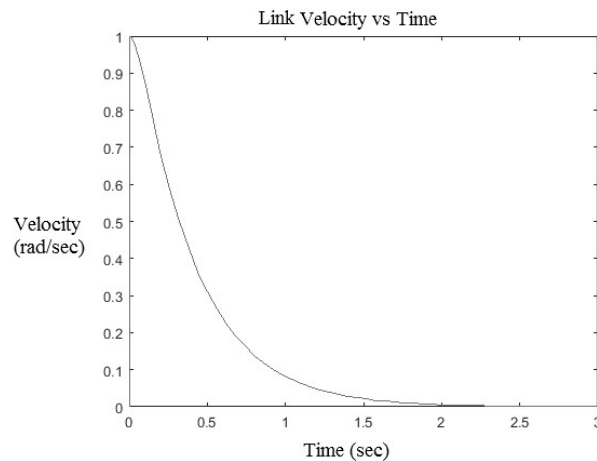


Figure 3.1: Link Velocity vs Time (Keeping damping and Stiffness Constant)

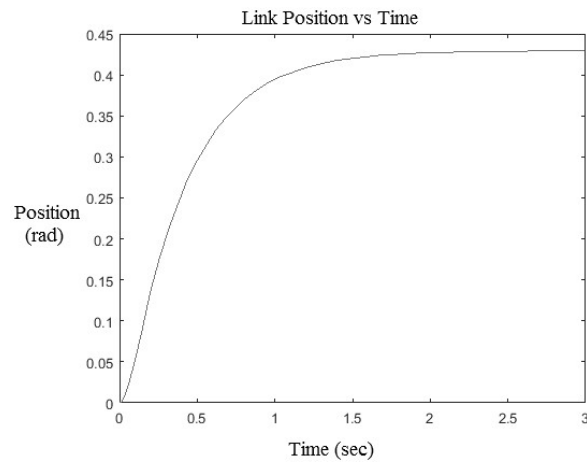


Figure 3.2: Link Position vs Time (Keeping damping and Stiffness Constant)

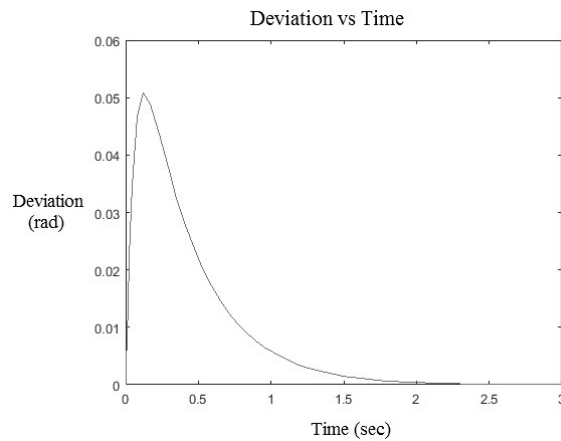


Figure 3.3: Deviation  $r - q_2$  vs Time (Keeping damping and Stiffness Constant)

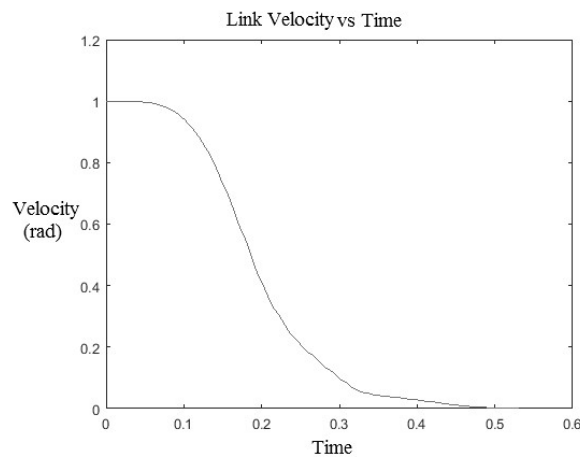


Figure 3.4: Link Velocity vs Time (Varying damping and Stiffness Constant)

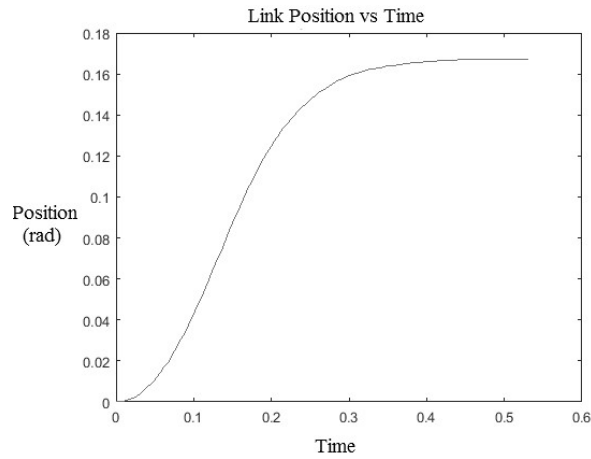


Figure 3.5: Link Position vs Time (Varying damping and Stiffness Constant)

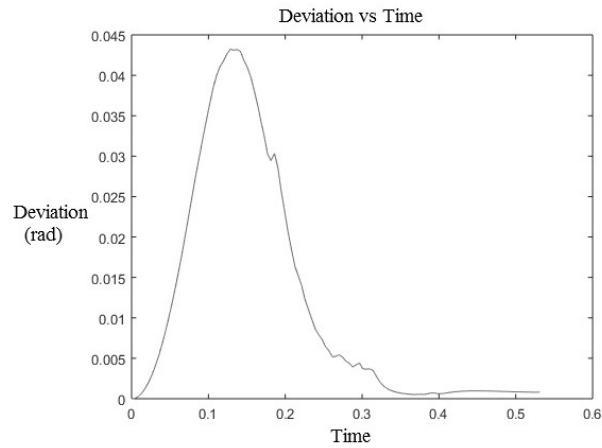


Figure 3.6: Deviation  $r - q_2$  vs Time (Varying damping and Stiffness Constant)

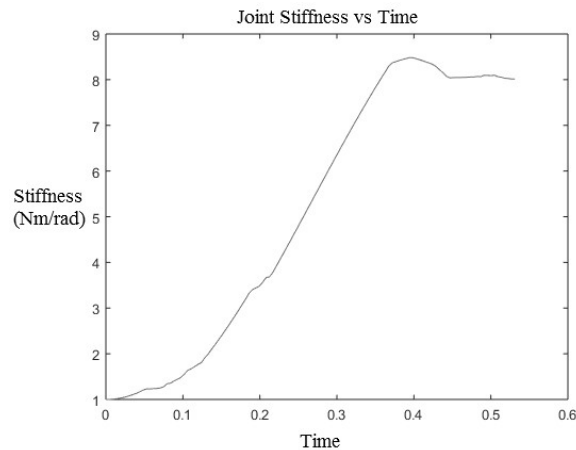


Figure 3.7: Link Stiffness vs Time (Varying damping and Stiffness Constant)

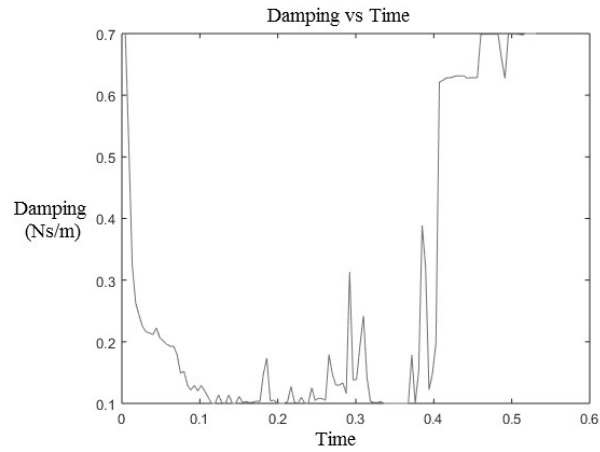


Figure 3.8: Damping vs Time (Varying damping and Stiffness Constant)

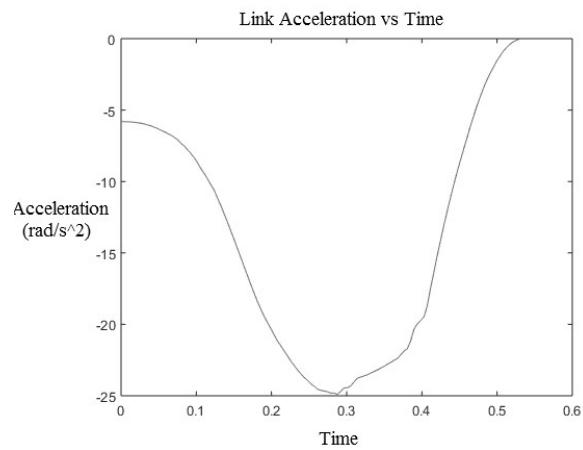


Figure 3.9: Acceleration vs Time (Varying damping and Stiffness Constant)

### 3.4 Conclusion from Simulation Results

It can be observed that the deviation  $r - q_2$  remains almost the same in both the cases. But, the time in which the velocity of the link goes to zero is much less when optimal control is used. It can be observed that that the stiffness increases with time, causing an increased decelerating force on the link, thus stopping it in lesser time. This also leads to a lesser deflection of the link from its initial position. In sum, varying the stiffness and damping of the controller provides better performance.



# Chapter 4

## Discussion and Future Work

This work studied the controller design for a catching task realized using a Variable Stiffness Actuator. An object moving with an unknown velocity is brought to rest. This is achieved by implementing a virtual damper in the controller.

Two controllers were compared in a simulation study. The first one, kept constant, the stiffness of the VSA and the damping coefficient of the virtual damper during the course of catching. The second varied the stiffness and the damping coefficient during the course of catching.

It was observed that varying the stiffness and damping, the link was brought to rest in a lesser time and the deviation of the link from its initial position was greatly reduced. Thus, providing better performance.

As of now, the results are presented using simulation tests. Experimental test of the optimal controller can form a part of the future work.

# Bibliography

- [1] A. Albu-Schäffer et al. “Dynamic Modelling and Control of Variable Stiffness Actuators”. In: *Proceedings of the IEEE International Conference on Robotics and Automation*. 2010, pp. 2155–2162.
- [2] B. Vanderborght et al. “Variable impedance actuators: A review”. In: *Robotics and autonomous systems* 61 (12 2013), pp. 1601–1614.
- [3] B. Vanderborght et al. “Variable impedance actuators: Moving the robots of tomorrow”. In: *Proceedings of the IEEE/RSJ International Conference on Intelligent Robots and Systems*. 2012, pp. 5454–5455.
- [4] Berthold Bäuml, Thomas Wimböck, and Gerd Hirzinger. “Kinematically Optimal Catching a Flying Ball with a Hand-Arm-System”. In: *Proceedings of the IEEE/RSJ International Conference on Intelligent Robots and Systems*. 2010.
- [5] Giorgio Grioli et al. “Variable stiffness actuators: The user’s point of view”. In: *International Journal of Robotics Research* 34.6 (2015), pp. 727–743.
- [6] S.S. Groothuis, S. Stramigioli, and R. Carloni. “Lending a helping hand”. In: *IEEE Robotics and Automation Magazine* 20.1 (2013), pp. 20–29.
- [7] S.S. Groothuis et al. “The Variable Stiffness Actuator vsaUT-II: Mechanical Design, Modeling and Identification”. In: *IEEE/ASME Transactions on Mechatronics* 19.2 (2014), pp. 589–597.
- [8] Kenneth Holmström. “The TOMLAB optimization environment in Matlab”. In: (1999).
- [9] Kevin Kemper et al. “Optimal Passive Dynamics for Physical Interaction: Catching a Mass”. In: *Actuators 2* (2013), pp. 45–58.
- [10] J. Kumble. *Controller Design of a Variable Stiffness Joint for Catching a Moving Object*. BSc report 036RaM2015. University of Twente, Dec. 2015.
- [11] C. Ott et al. “On the Passivity-Based Impedance Control of Flexible Joint Robots”. In: *IEEE Transactions on Robotics* 24.2 (2008), pp. 416–429.

- [12] F. Petit and A. Albu-Schäffer. “State Feedback Damping Control for a Multi DOF Variable Stiffness Robot Arm”. In: *Proceedings of the IEEE International Conference on Robotics and Automation*. 2011, pp. 5561–5567.
- [13] Naoki Uchiyana, Shigenori Sano, and Kazuaki Ryuman. “Adaptive control of a robotic manipulator for soft catching of a falling object”. In: *JSME Mechanical Engineering Journal* 2.3 (2015), pp. 1–12.
- [14] S Wolf et al. “Variable stiffness actuators: Review on design and components”. In: *IEEE/ASME Transactions on Mechatronics* 21.5 (2016), pp. 2418–2430.